Pergamon

Acta mater. 49 (2001) 3289–3293

Acta MATERIALIA

www.elsevier.com/locate/actamat

A.C. CONDUCTIVITY BEHAVIOR OF A HOT PRESSED [$PbTiO_3$–$PbZrO_3$–$PbCuNbO_3$] FERROELECTRIC CERAMIC

A. PELÁIZ BARRANCO[1], F. CALDERÓN PIÑAR[1], O. PÉREZ MARTíNEZ[1], E. TORRES GARCÍA[1] and A. HUANOSTA-TERA[2]†

[1]Facultad de Física-Instituto de Materiales y Reactivos, Universidad de La Habana, San Lázaro y L. Vedado, La Habana 10400, Cuba and [2]Instituto de Investigaciones en Materiales, Universidad Nacional Autónoma de México, Apartado Postal 70-360, Mexico D.F. 04510, Mexico

(Received 14 December 2000; received in revised form 27 April 2001; accepted 10 May 2001)

Abstract—The temperature dependence of electric parameters of the sintered compound $PbZr_{0.5}Ti_{0.44}(Cu_{1/4}Nb_{3/4})_{0.06}O_3$ + 0.5 mol% MnO_2 was investigated using a.c. measurements. The temperature dependence of the a.c. conductivity in the vicinity of T_c is highly non-linear with a local maximum in conductivity observed at that temperature. The total conductivity $\sigma_t(\omega)$, as a function of frequency, exhibits a power law dependence ($\sigma_0 + A\omega^s$), whose exponent s is maximized at the ferro–paraelectric transition. © *2001 Acta Materialia Inc. Published by Elsevier Science Ltd. All rights reserved.*

Keywords: a.c. Conductivity; Hot pressing; Ceramic; Ferroelectricity; Dielectric permittivity

1. INTRODUCTION

The motion of charge carriers in ceramic materials can be difficult to describe due to the complex dynamic processes involved. However, conductivity can be described in an acceptable way by considering a.c. and d.c. electrical properties. Actually, impedance, admittance, permittivity or complex modulus are used world wide to analyze frequency dispersion data from a variety of physical systems [1]. It was found appropriate to use a combination of these formalisms to study the electrical properties of hot pressed polycrystalline $PbTiO_3$–$PbZrO_3$–$PbCuNbO_3$, which was modified by adding 0.5 mol% MnO_2. In this ferroelectric ternary system, copper and niobium replace the Zr^{4+} or Ti^{4+} species on the B site of the structure as hard and soft doping ions, respectively. This compound belongs to a complex ternary system (PZT), which has proved technological importance in electronics and electro-optics [2, 3]. Previous studies [4, 5] have shown a simple perovskite phase is formed and that the manganese enters in the lattice displacing Cu^+ ions (the copper and manganese ions occupy the same crystallographic site, the B-site, in the perovskite structure). In this paper, the a.c. conductivity behavior is studied and it is shown that the ferroelectric–paraelectric transition temperature, T_c, can be determined using a.c. measurements.

2. EXPERIMENTAL PROCEDURE

Samples with the composition $PbZr_{0.5}Ti_{0.44}(Cu_{1/4}Nb_{3/4})_{0.06}O_3$ + 0.5 mol% MnO_2 were prepared by hot pressing. Ceramic bodies were obtained from high purity reagents and the calcination and milling procedures were carried out simultaneously using a ball mill, which was kept at 600°C in air. Hot pressed ceramics were obtained at 1000°C, for 1h under a pressure of 6 MPa in air.

a.c. Impedance measurements were carried out using a Hewlett-Packard HP 4192A Impedance Analyzer controlled by a personal computer. Using organogold paste covered by a strip of gold foil, gold blocking electrodes were fabricated on opposite faces of a coin-shaped pellet (13 mm diameter and ~1 mm thickness). The pellet was attached to the Pt electrode wires of a conductivity cell, and this placed inside a well regulated vertical tube furnace. The frequency range studied was from 5 to 13 MHz and an applied voltage of 1 V was employed. The temperature range investigated was from 180 to 700°C in air. A thermocouple was placed close to the sample (3–4 mm) to measure accurate temperatures.

The hot pressing process yielded high density ceramic bodies as corroborated by scanning electron microscopy (Cambridge–Leica Steroescan 440). Plan-view microscopy of fractured ceramics indicated a

† To whom correspondence should be addressed. Tel.: +52 5622 4641; fax: +52 5616 1371.

E-mail address: dmmciim@servidor.unam.mx (A. Huanosta-Tera)

PII: S1359-6454(01)00205-1

grain size between 3 and 6 μm. The relatively uniform grain size distribution leads to reliable conductivity characterization.

3. RESULTS

3.1. a.c. Conductivity and d.c. behavior

Important dispersion phenomena cannot be considered if frequency independent data (d.c. measurements) are used to characterize the temperature dependence of the conductivity. A more detailed description is obtained using the dynamic conductivity method, $\sigma_T(\omega) = gY'$, where g is a geometric factor, given by the quotient: thickness of the sample/area of one electrode, $Y' = Z'/[(Z')^2 + (Z'')^2]$ is the real part of the admittance, and Z′ and Z″ are the real and imaginary parts of the impedance, respectively.

Figure 1, which plots log $\sigma_t(\omega)$ against $10^3/T$ at 1, 10, 100 kHz and 1 MHz, shows a marked dispersion in the conductivity, particularly around a critical temperature, identified from previous paper [6] as T_c. An increase in conductivity occurs around T_c, appearing as a very sharp maximum in each curve. The apparent increase in the conductivity is attributed to the increased polarizability of the material around T_c.

At temperatures well above T_c, the conductivity data tends to fall onto a straight line. This is typical behavior of the d.c. component in curves as those in Fig. 1 [7]. Thus, the solid line indicated in Fig. 1 suggests the approximate trend of the d.c. conductivity. The associated activation energy was calculated as 1.60±0.03 eV, which compare properly with previous results [8].

3.2. Power law dependence of conductivity

Figure 2 shows the log $\sigma_T(\omega)$ plotted as a function of log ω at two selected temperatures, 420 and 700°C, exemplifying the general behavior. Generally speaking, as a function of temperature the curves log $\sigma_T(\omega)$ versus log ω exhibit two dispersive components, typical of relaxation process. At low temperatures, dispersion dominates almost the total frequency interval. While frequency independent behavior is the main component at the highest temperatures. This means, from low to high temperature the dispersive components shift toward the high frequency region, first appearing as a moderate frequency independent component at the low frequency region, and then at the highest temperatures (close to 700°C) the curves become almost completely frequency independent, as illustrated in Fig. 2.

The curve at 420°C exhibits the first dispersive stage at around 1 kHz, which come from electrode effects, whereas the second one at around 1000 kHz, is associated with bulk phenomena, as it will be justified latter. The arrow indicates the crossover frequency associated with bulk phenomena.

At the 700°C curve in Fig. 2, additional dispersion is observed above 10^6 Hz, this is considered as dispersion due to detection limits of the used equipment.

This type of behavior has been observed in a wide variety of materials [9] over several decades of frequency. Jonscher [10] has proposed the relation:

$$\sigma_T(\omega) = \sigma_0 + A\omega^s \tag{1}$$

to describe such behavior. In this power law relation, σ_0 is considered the d.c. component, which is tem-

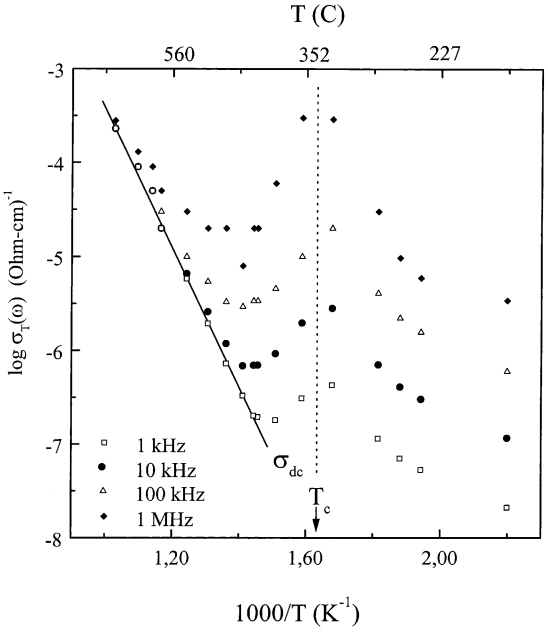

Fig. 1. $\sigma_T(\omega)$ plotted in Arrhenius fashion at selected frequencies. The straight line represents the σ_{dc} as limit of the a.c. conductivity at higher temperatures and low frequencies.

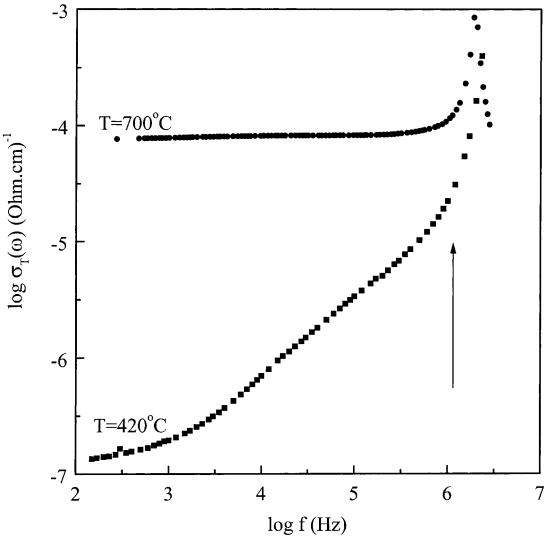

Fig. 2. Frequency dependence of the dynamic conductivity at 420°C.

perature dependent. The term $A\omega^s$ accounts for the dispersion phenomena, A is a temperature dependent parameter which determine the magnitude of the dispersion, the exponent s is also temperature dependent [11], with $0<s<1$.

Assuming this type of behavior, s was calculated and its temperature dependence was studied (Fig. 3). This parameter shows a maximum of about 0.83, near $T = 343°$, after which, it decreases as the temperature rises.

3.3. Dielectric permittivity

One of the most common procedures to find the ferroelectric–paraelectric transition temperature is to determine the maximum of the permittivity as a function of temperature. In order to support the above results, obtained by a.c. measurements, the dielectric permittivity is plotted as a function of temperature for a few frequencies (1, 10, 100 kHz, and 1 MHz). The frequency dependent permittivity was obtained by:

$$\varepsilon'(\omega) = (g/\varepsilon_0)\{\omega Z''[1 + (Z'/Z'')^2]\}^{-1} \qquad (2)$$

where $\varepsilon_0 = 8.854\times10^{-14}$ F/cm, and g as defined before.

Figure 4 shows the 1 kHz data which exhibits a maximum at 343°C, the Curie temperature. Above this temperature, the curve seems to follow a characteristic Curie–Weiss behavior. However, at low frequencies, there is an increasing tendency for the values of $\varepsilon'(\omega)$ to become higher at above 500°C, as commonly occurs in non-ferroelectric ceramics [12]. All plots of $\varepsilon'(\omega)$ against T, follow the same trend. This result confirms that the T_c observed in Fig. 1, and temperature corresponding to the maximum value of s, in fact correspond to the ferroelectric–paraelectric transition temperature.

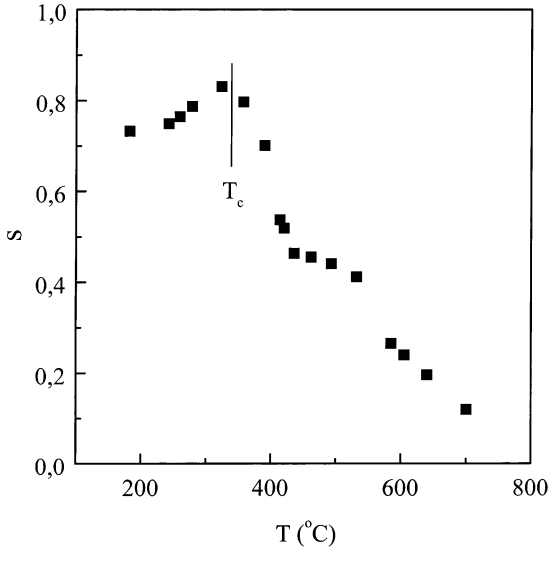

Fig. 3. Temperature dependence of the s parameter.

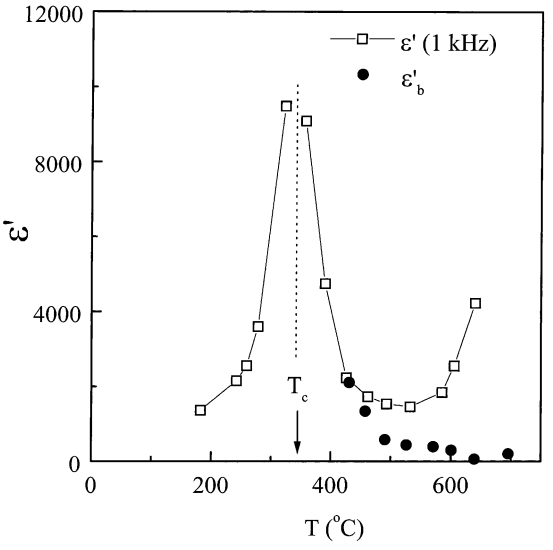

Fig. 4. Temperature dependence of the permittivity for 1 kHz (open squares) and data (solid circles) obtained from bulk capacitances ($\varepsilon'_b = gC_b/\varepsilon_0$).

3.4. Impedance data and bulk characteristics

It is also known that the electrical characteristics of a material are a consequence of many interrelated factors, whose evaluation and identification represents a major problem. However, to good approximation, such characteristics can be closely represented by an equivalent circuit, which may be suggested by direct observation of the resultant impedance plots. At temperatures below 400°C the studied compound showed only a fraction of an arc in the impedance plots. At temperatures above 450°C a very well resolved semicircle appears, and at temperatures around 600°C a poorly resolved second arc begins to appears. Figure 5 shows the impedance representation of the electrical

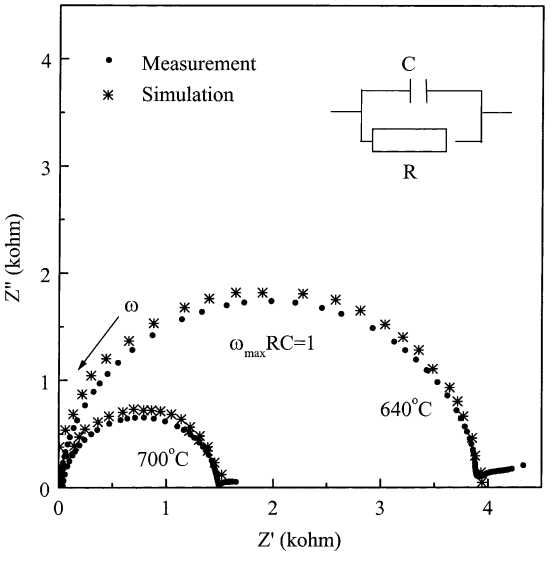

Fig. 5. Electrical response for a couple of selected temperatures in its impedance representation. Both measured and simulated curves using the proposed equivalent circuit are shown.

response for two temperatures. A parallel *RC* equivalent circuit can be associated to the full experimental semicircle. The *R* and *C* parameters were calculated in the usual way [1], i.e., the resistance (*R*) was calculated from the low frequency intercept of the semicircle on the real Z' axis and the capacitance (*C*) values were obtained from the maximum condition of the semicircle $\omega_{max}RC = 1$, where $\omega_{max} = 2\pi f_{max}$, f_{max} being the frequency at the maximum of the semicircle. Although all calculation can be made in a reliable way just by direct observation on the impedance plots, we have also used the NLLS-fit program [13] to support our results. In Fig. 5, both measured and simulated curves using the proposed equivalent circuit are shown.

The parallel *RC* mesh assigned to the full semicircle is in fact describing the electrical bulk characteristics, this is concluded because the calculated capacitances are in the order of pF, which is typical value for bulk behavior [14]. As the frequency dispersion for the bulk occurs at the high frequency region at every temperature, then the dispersive stage pointed with an arrow in Fig. 2 is due to bulk behavior. Unfortunately, reliable C_b (bulk capacitance) values were only obtained above T_c. This is the main reason we do not present the temperature dependence of C_b to determine T_c. In Fig. 4, these results are shown as solid circles ($\varepsilon'_b = gC_b/\varepsilon_0$).

Using the obtained *R* values, via impedance plots, the temperature dependence of the bulk conductivity, calculated from $\sigma_b = g/R$ (*g* already defined), exhibits a quasi-linear behavior (Fig. 6) from 400 to 700°C, which can be described by $\sigma = \sigma_0 \exp^{-E_{\sigma_b}/kT}$, where σ_0 is a pre-exponential factor, $E_{\sigma b}$ is the activation energy for bulk conduction, and *k* is the Boltzmann constant. The associated activation energy, $E_{\sigma b}$, was 1.50±0.02 eV. This value is compatible with that calculated for the d.c. component in Fig. 1. So, in a good approach, we can conclude that in this case the conductivity in Fig. 6 is the d.c. conductivity.

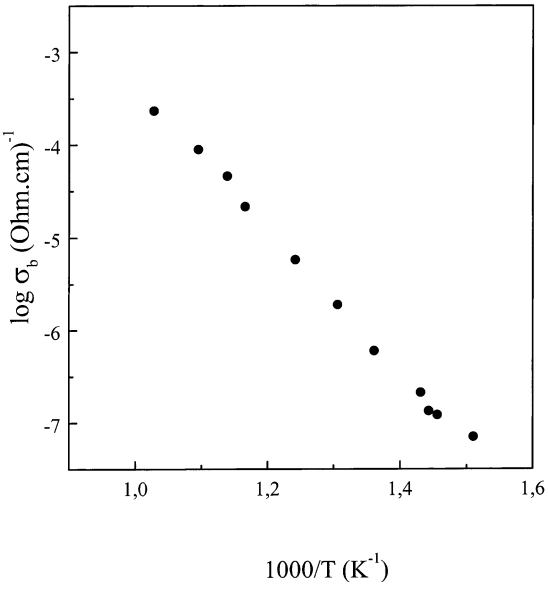

Fig. 6. Temperature dependence of the bulk conductivity.

4. DISCUSSION

Up to around 600°C, the impedance curves show neither a grain boundary response, nor the presence of a spike at the low frequency region. This may indicate that electrons are the main charge carrying species. Nevertheless, at higher temperatures, a small second arc appears at the low frequency regions on the impedance curves, whose presence suggests that a small ionic component is present. This is particularly confirmed by the capacitance value calculated at the very low frequency tail, which is of the order of μF. That capacitance must be associated with a charge layer at the electrode region [14], which arises due to ionic migration. This also indicates that the dispersion at low frequencies (1 kHz) in Fig. 2 describes electrode phenomena.

Even when normal reported trends of the *s* parameter [15] indicated it as a constant or exhibiting a monotonic rise with decreasing temperature, in the present work it is shown that this parameter reflects the ferroelectric–paraelectric transition of the studied compound by exhibiting a maximum value. Similar behavior of *s* has been reported in Reference [16]. That behavior in relation (1) can be described by the jump relaxation model by Funke [17], which implies a physical meaning of the exponent *s* [18]. That is, *s* describes the ratio: backhop rate to the site relaxation rate.

Since in Fig. 3, we have shown that, from low to high temperature, *s* increases up to T_c, then following the model in Reference [18], either of the following two possibilities may increase the mentioned ratio. First, there are increasing Coulombic interactions between mobile ions; or second, due to rearrangement of neighboring ions, the value of the shift of a site potential minimum to the position of the hopping ion, i.e. the site relaxation rate, is diminishing. As it is known that below T_c the ferroelectric system is reaching an ordered state, we believe that the second possibility may be favored when the temperature is below T_c. Then, as a function of temperature s grows at this stage, see Fig. 3.

In contrast, above T_c, the cooperative distortion responsible for ferroelectricity is eliminated, and the relaxation rate could increase because the stiffness of the crystalline structure has changed. Moreover, subsequent increase of the Coulombic repulsive interactions between mobile ions causes a decreases of the backhop rate, and then *s* decreases. Therefore, the combination of configurational and electrostatic phenomena associated with ferro–paraelectric transitions should influence, as observed above, the behavior of *s*.

5. CONCLUSIONS

The dielectric response of a well formed ferroelectric ceramic, sintered by hot pressing is reported. Electric conductivity ranging approximately from 10^{-8} to 10^{-4} (Ohm-cm)$^{-1}$ is observed, typical of semiconductor materials. The total conductivity $\sigma_T(\omega)$, as a function of frequency follows a power law ($\sigma_0 + A\omega^s$), whose exponent *s* exhibits the ferro–paraelectric transition when plotted against temperature. This implies that the temperature dependence of the s parameter is a fundamental response. Results indicate that, in the studied compound, collective effects determine the a.c. and d.c. components, and necessarily complex many body interactions must be involved.

Acknowledgements—The authors wish to thank Dr José Cháves C. for helpful discussion, I.Q. Leticia Baños, M. and C. José Guzmán M. for technical help, and TWAS for partial financial support.

REFERENCES

1. Macdonald, J. R., (ed.), *Impedance Spectroscopy*. Wiley, New York 1987.
2. Jaffe, B., Cook, W. and Jaffe, H., *Piezoelectric Ceramics*. Academic Press, London, 1971.
3. Fernández, J. F., Durán, P. and Moure, C., *Bol. Soc. Esp. Cer. Vidr.*, 1993, **31**(1), 5.
4. Peláiz Barranco, A., Calderón Piñar, F., Pérez Martínez, O. and Torres García, E., *J. Eur. Ceram. Soc.*, 2001, **21**(4), 523.
5. Torres García, E., Peláiz Barranco, A., Vázquez, C., Calderón Piñar, F. and Pérez Martínez, O., *Thermochim. Acta*, 2001, **39**(1-2), 372.
6. Calderón, F., Pérez, O., Peláiz, A. and Font, R., *Rev. Mex. De Fís.*, 1996, **42**(1), 82.
7. Lee, B. S., Lim, J. F., Liu and Nowick, A. S., *Sol. State Ionics*, 1992, **53–56,** 831.
8. Peláiz Barranco, A., Calderón Piñar, F., Pérez Martínez, O., De Los Santos Gerra, J. and González Carmenate, I., *J. Eur. Ceram. Soc.*, 1999, **19**(15), 2677.
9. Jonscher, A. K., *Dielectric Relaxation in Solids*. Chelsea Dielectrics Press, London, 1983.
10. Jonscher, A. K., *Nature*, 1977, **267**, 673.
11. Almond, D. P., West, A. R. and Grant, R. J., *Sol. State Commun.*, 1982, **44**, 277.
12. Flores-Ramirez, R., Huanosta, A., Amano, E., Valenzuela, R. and West, A. R., *Feroelectrics*, 1989, **99**, 195.
13. Boukamp, B. A., Equivalent circuit (equiver. pas), University of Twente, Department of Chemical Technology, The Netherlands, 1988.
14. Irvine, J. T. S., Sinclair, D. C. and West, A. R., *Adv. Mater.*, 1990, **2**, 132.
15. Elliott, S. R. and Henn, F. E. G., *J. Non-Crystalline Solids*, 1990, **116**, 179.
16. Peláiz-Barranco, A., Gutiérrez-Amador, M. P., Huanosta, A. and Valenzuela, R., *Appl. Phys. Lett.*, 1998, **73**(14), 2039.
17. Funke, K., *Prog. Solid State Chem.*, 1993, **22**, 111.
18. Mizomoto, K. and Hayashi, S., *Sol. State Ionics*, 2000, **127**, 241.